Colloid Polym Sci (2002) 280: 900–907
DOI 10.1007/s00396-002-0700-5

ORIGINAL CONTRIBUTION

Changqi Sun
Yoh Sano
Hiroshi Kashiwagi
Masaharu Ueno

Characterization of aggregate structures of phospholipid in the process of vesicle solubilization with sodium cholate using laser light scattering method

Received: 5 December 2001
Revised: 5 March 2002
Accepted: 13 March 2002
Published online: 23 May 2002

C. Sun · H. Kashiwagi · M. Ueno (✉)
Faculty of Pharmaceutical Sciences,
Toyama Medical and Pharmaceutical
University, 2630 Sugitani,
Toyama 930-0194, Japan
E-mail: mueno@ms.toyama-mpu.ac.jp
Tel.: +81-76-4347565
Fax: +81-76-4345050

Y. Sano
Faculty of Pharmaceutical Sciences,
Setunan University,
45-1 Nagaotoge-machi,
Hirakata 573–0101, Japan

Abstract The aggregate structures formed during vesicle solubilization by sodium cholate, and their properties, were characterized by static laser light scattering (SLS) and electrophoretic light scattering (ELS) methods. The change in dissymmetry value Z_{45} was observed by examining the regions of vesicles and micelles. The angular light scattering intensity data could be fitted with a modified shell model for the vesicles and a hollow cylinder model for the mixed micelles. In the case of the vesicles, the scattering curves were fitted with a spherical shell model by introducing the interparticle scattering factor S(q) and taking into account the intervesicle positional correlations, which is a function of the fractal dimension (D) and the interparticle correlation length (L). On the basis of the physical meanings of the fractal dimension and interparticle correlation length, the molecular packings of the membrane and the repulsive interaction between the vesicles were analyzed. Furthermore, using electrophoretic light scattering (ELS) the zeta potentials on the mixed vesicles were found to increase with the molar ratio (Re) of sodium cholate to egg yolk phosphatidylcholine (EggPC) in the membrane. It is suggested that the electrostatic properties of the vesicles result in repulsive interaction which is responsible for no fusion of the mixed vesicles. In addition, in the transition from vesicles to micelles, a cylinder-like micelle appeared as an intermediate structure.

Keywords Vesicle solubilization · Angular light scattering · Interparticle scattering factor S(q) · SUV* fusion · Cylindrical micelle

Introduction

The mechanisms of vesicle solubilization by detergent have been extensively studied by various experimental techniques–fluorimetry, DSC, ESR, NMR and many other methods [1, 2, 3, 4, 5, 6, 7]. The aggregate structure has also been examined by small-angle neutron scattering, small-angle X-ray scattering, and cryo-transmission electron microscopy [8, 9, 10, 11]. Recently, a four-stage model, instead of a three-stage model, for the mechanism of vesicle solubilization has been proposed. This involves: 1) the distribution of detergent between water and lipid phase resulting in mixed vesicles; 2) an increasing concentration of detergent leads to small, nearly detergent-saturated vesicles, or SUV*, which are distinguished in property from SUV prepared by sonication; 3) when a critical molar ratio of detergent/lipid is reached, a slight increase of detergent concentration causes the vesicles to transform into the intermediates, large micelles of disk or cylindrical structures; 4) lastly, the intermediates disappear and detergent-rich micelles are formed [14, 17]. Although a number of studies have

been corroborated in the scheme of micelle-vesicle transition, the structures and properties of intermediates in the transition are still unclear [12, 13, 14, 15, 16, 17].

Investigations on the micelle-vesicle transition in the EggPC/sodium cholate system revealed that the small vesicles containing a large amount of sodium cholate, or SUV*, could not fuse to increase their sizes, contrasting with SUV* containing octylglucoside or CHAPS (3-[(3-cholamidopropyl)dimethylammonio]-1-propanesulfonate) [16, 17]. This fusion has been related to a size growth in the formation of large vesicles upon the detergent removal [18]. It was proposed that for the SUV* containing sodium cholate, no fusion event takes place because of electrostatic repulsion due to an anionic detergent, leading to small vesicle formation upon detergent removal [17]. However, no further detailed analysis has been made of the changes in surface potential of the vesicles in response to the addition of sodium cholate.

The main purpose of the present paper is to understand the structural transitions and the forces that hinder the SUV* fusion from a thermodynamic point in the vesicle solubilization by sodium cholate. The methods used were static light scattering (SLS), electrophoretic light scattering (ELS), and freeze-fracture electron microscopy. The measurements were carried out at a fixed concentration of about 5 mM of EggPC and at a series of detergent concentrations. The patterns of scattered light spectra were used to elucidate the aggregate structures and the vesicle properties. At the first step in this study, the regions of vesicles and micelles in the solubilization process were examined in term of the changes in the dissymmetry value Z_{45} (defined by the scattering intensity ratio at two angles R_{45} and R_{135}). The scattered light intensities for vesicles were well fitted with the spherical shell model by introducing the interparticular structure factor S(q). This assumes the interparticle positional correlation as the interparticle structure factor and is a function of the fractal dimension D and the interparticle correlation length L. This approach could be helpful in observing the changes in the vesicle behavior as a function of the molar ratio (Re) of sodium cholate to EggPC in the membrane. In addition, the electrophoretic mobility of those vesicles was measured as zeta potential. The results from SLS support the theory that in vesicle solubilization by sodium cholate, SUV* could not fuse to grow in size due to the surface charges and that the cylindrical micelles appeared as an intermediate between the vesicles and micelles.

Theoretical

In the present work, the shape and size of the vesicles and micelles were determined by comparing the experimental angular scattered light profiles with the calculated values for suitable models. The theoretical equations of the shape factor, P(q), are given as a function of scattering angle for various models such as shell and hollow cylinder.

For a vesicle giving two concentric spherical shell models [19]:

$$P(q) = \left[1\Big/\left(R^3 - Ri^3\right)^2\right]\left[R^3F(qR) - Ri^3F(qRi)\right]^2 \tag{1}$$

$$q = 4\pi \sin(\theta/2)/\lambda \tag{2}$$

$$F(qR) = 3(\sin qR - qR\cos qR)\Big/(qR)^3 \tag{3}$$

Where λ is the wavelength of laser light in suspension (nm); R is outer radius and Ri inner radius; the phospholipid bilayer thickness is assumed to be 4.5 nm according to Chang and Colbow [20].

The experimental values almost agreed well with the theoretical curve in the higher q regions, but sometimes did not in the lower q regions. The deviation of experimental values from theoretical ones in the lower q region might be due to the interparticular structure factor S(q). S(q) is an interparticle structure factor taking into account the interparticular positional correlation and is defined in terms of particle pair correlation function g(R) as a function of the fractal dimension of the particular distribution in space D and the particle-particle correlation length L [20, 21, 22]

$$S(q) = 1 + N\int_0^\infty 4\pi R^2[\sin(qR)/qR]g(R)dR \tag{4}$$

$$g(R) = (D/4\pi N)\left(1/R^D\right)R^{(D-3)}\exp(-R/L) \tag{5}$$

where N is number density of vesicles in suspension. In this case, the scattering intensity profiles are proportional to P(q)S(q).

For a hollow cylinder of diameter $2R$ and height H [23]

$$P(q) = \int_0^1 F\left[q, R\left(1-X^2\right)^{1/2},\ R_i\left(1-X^2\right)^{1/2}\right]^2 S^2(qHX/2)dX \tag{6}$$

$$F(q,R,R_i) = \left[1/\left(1-r^2\right)\right]\left[A(qR) - r^2A(qR_i)\right] \tag{7}$$

$$r = R_i/R \tag{8}$$

$$S(X) = \sin(X) \tag{9}$$

$$A(qR) = 2J_1(qR)/(qR) \tag{10}$$

Where J_1(q R) is the first order Bessel function.

Experimental

Vesicle solubilization by sodium cholate

EggPC was obtained from Nihhon Yushi, Japan. Sodium cholate was from Nacalai Tesque, (Kyoto, Japan). The samples were used without further purification.

Egg PC was dried overnight at vacuum after the removal of $CHCl_3$/MeOH and suspended at a concentration of 25 mM in an appreciate buffer system of 150 mM NaCl and 20 mM TES (pH, 7.0). The SUV suspension was prepared by sonication using a probe-type sonicator at 4 °C, then diluted to 10 mM with the buffer as a stock SUV suspension.

The solubilization of vesicles by detergent was performed by adding a series of concentrations of detergent solutions to SUV suspensions (prepared by sonication with a syringe) while stirring the suspensions. The phospholipid concentrations were fixed at 5 mM. The solubilization process of the small vesicles was at first estimated by turbidity and size measurements. Turbidity was measured at 350 nm by a UV spectrophotometer (UV-160, Shimadzu, Japan) and the size by a quasielastic light scattering (QLS) apparatus (LPA-3000, Otsuka electronics, Japan).

The molar ratio (Re) of sodium cholate to EggPC in the membrane was directly measured by equilibrium dialysis according to the method previously reported [24]. Sodium cholate concentration was determined by monitoring radioactivity of ^{14}C-sodium cholate using an Aloka LSC-5200 liquid scintillation system. Phospholipid concentration was determined as phosphorous according to Ames [25].

The freeze-fractured specimens of vesicles and micelles were prepared according to the method previously reported [26] using a freeze-fracture apparatus (EIKO FD-2A). Electron micrographs were taken with a JEOL JEM-200 CX electron microscope.

Measurements of angular light scattering

Measurements of the light scattered intensity at various scattering angles were carried out with a modified Ellipsometer, an automatic light scattering analyzer AEP-100 (Shimadzu Co., Ltd., Japan), at 20°C [27, 28, 29]. The linearly polarized monochromatic incident light passed through the cylindrical scattering cell and the light scattered at scattering angle θ was detected through the linear analyzer by a photomultiplier in a telescopic arm that can rotate from 45° to 135° using a stepping motor. A wavelength of 488 nm was used. The samples were made optically clean by filtering with a Millipore filter (pore size, 0.45 μm).

Taking into consideration that diluting the mixed vesicles or micelles of detergent and phospholipid affected their shapes and properties [12], the SLS measurements for those mixed vesicles or micelles were performed based on the angular dependence of scattered light intensity and analyzed according to the Zimm plot method.

Measurements of zeta potential

Electrophoretic light scattering apparatus (ELS-8000/6000, Otsuka Electronics, Japan) was used to determine the electrophoretic mobility of the vesicles or micelles. The electrophoretic mobilities of the particles were measured 3–5 times for each sample. The measurements were made in the electric fields applied in the direction of gravity and in the opposite direction and the mobility was given by the arithmetic mean of mobility values in the two directions. The movement of particles was analyzed by the frequency distribution of light scattered from the suspensions.

The mobility was converted to zeta potential through the Smoluchowski equation as follows:

$$Up = \varepsilon\zeta/(4\pi\eta) \tag{11}$$

where Up is mobility, ξ is zeta potential, ϵ is dielectric constant, η is coefficient of viscosity.

Results and discussion

Partition equilibrium of detergent between the membrane phase and the water phase

Since for elucidation of the solubilization process it is more important to know the detergent concentration in the membrane phase than the overall detergent concentration, we performed the partition experiment of sodium cholate between membrane and water phases as shown in Fig. 1. The ordinate represents the molar ratio of sodium cholate to phospholipids in the membrane phase in partition equilibrium and the abscissa represents the total detergent concentration. The molar ratio Re is given by

$$Re = C_b/C_p \tag{12}$$

C_b is the concentration of detergent in the membrane and C_p is the concentration of EggPC.

In the low concentration region, the plot gave an almost linear relation. At molar ratios above 0.15, the slope became lower, showing a small increase of the incorporation of sodium cholate into the vesicles. This small increase might be due to the establishment of electrostatic potential on the vesicle surface because sodium cholate is an anionic detergent. Over 0.25, an abrupt increase of the molar ratio Re was observed to accompany vesicle destruction, or the formation of mixed micelles, as shown in Fig. 1.

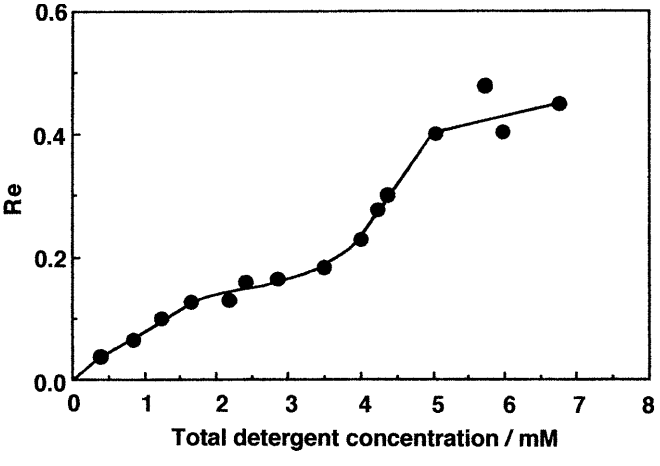

Fig. 1 Partition equilibrium of sodium cholate between the membrane phase and the water phase at 25 °C. The total concentration of the detergent (C_t) is represented by the molar concentration and that in the membrane phase (Re) by the molar ratio. The phospholipid concentration is about 5 mM and NaCl concentration is 150 mM

Changes in suspension turbidity and vesicle size during the solubilization process

Figure 2 shows the changes in apparent size and turbidity by adding sodium cholate to SUV suspensions. Below the critical Re of 0.25, sodium cholate was distributed into the vesicle bilayers and no significant change in turbidity and apparent size was found. At the critical point of Re = 0.25, the freeze-fracture electron microscopic appearance of the suspension showed the morphology of small vesicles, indicating that vesicle structure remained. Beyond this point a slight increase in the detergent content of the vesicles caused a drastic increase in turbidity, indicating a change in the aggregate structures, that is, the vesicles were transformed into the intermediate, an aggregate structure between the vesicles and mixed micelles. Over Re = 0.45 the suspensions became optically transparent and the intermediates were converted completely into mixed micelles.

Observing the process of vesicle solubilization by static light scattering

Figure 3 shows the relationship between Z_{45} (ratio of the scattered light intensities at 45° and 135°) and molar ratio Re. Since the intensity of scattered light decreased due to an interference effect, the dissymmetry factor Z_{45} is generally larger than one when the particle size is larger than about 1/20 of the wavelength of irradiated laser light [30]. Below the critical point (Re = 0.25), the Z_{45} remained almost constant, independent of the Re increase. This indicates that the addition of sodium cholate did not affect the vesicles in either the size or shape, which is in accord with the results measured by QLS and turbidity shown in Fig. 2. Beyond the critical Re, the Z_{45} began to decrease while the apparent size did not change until Re = 0.3.Thus, the decrease in Z_{45} resulted mainly from the change in particle shape but not in particle size [22]. Because SUV* is a vesicle containing a great amount of detergent, the Re for SUV* can be estimated at about 0.25. In Fig. 4 the morphology of SUV* was further demonstrated by the freeze-fractured electron micrograph.

The present experiments were carried out using serial concentrations of sodium cholate at a fixed EggPC concentration (5 mM). The samples were measured at intervals of 24 h within the two days required to reach equilibrium. Figure 5 shows the scattering patterns of the samples after 24 h, where I(q) shows the ratio of the scattered light intensity at various scattering angles to that at 135°. With an increasing incorporation of sodium

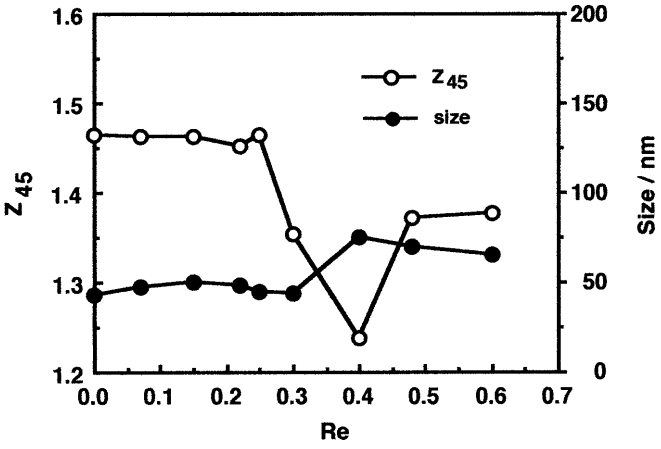

Fig. 3 The dissymmetry factor Z_{45} and apparent size as a function of the molar ratio (Re) in the solubilization of SUV by sodium cholate

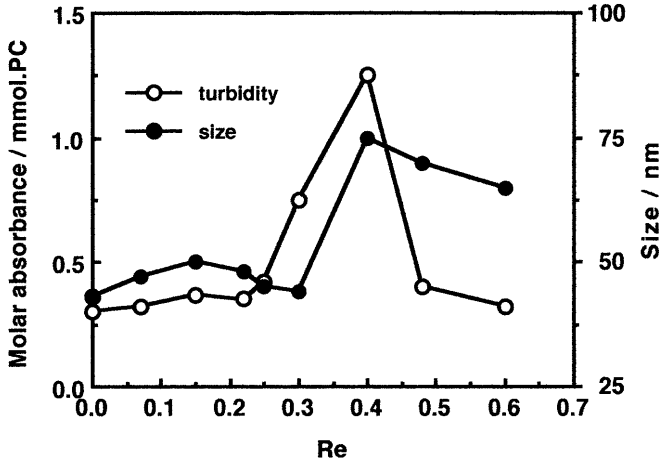

Fig. 2 Turbidity and apparent size as a function of the molar ratio (Re) in the vesicle solubilization by sodium cholate. The suspensions were incubated for 24 h at 25 °C. Apparent sizes were measured by QLS

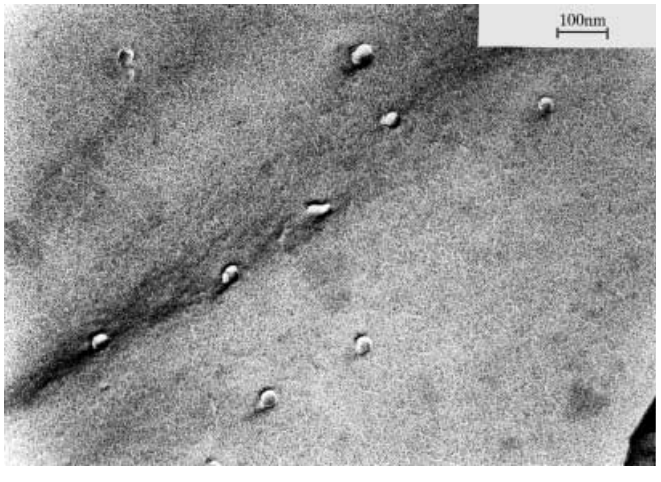

Fig. 4 Freeze fractured electron micrograph of SUV* at Re = 0.25

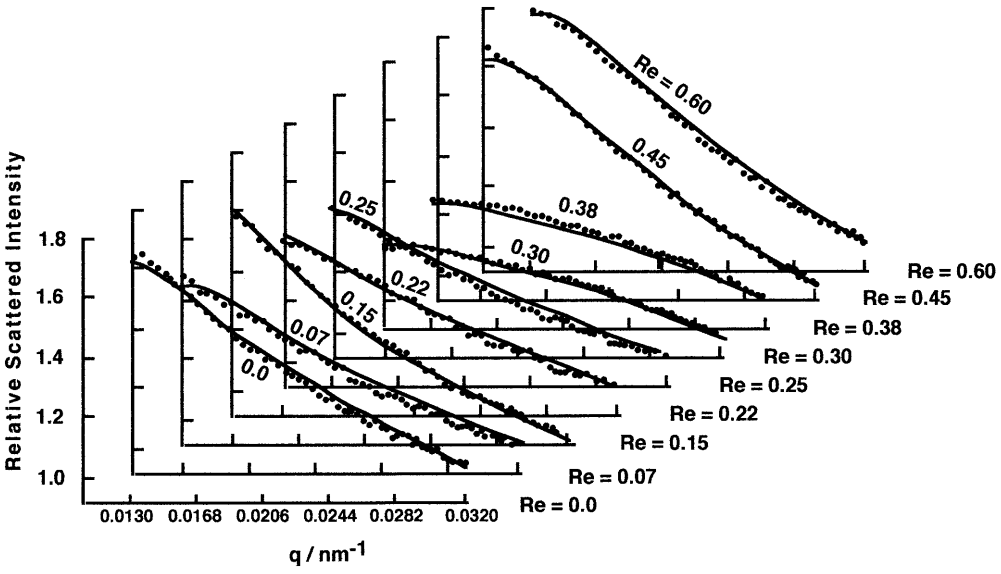

Fig. 5 Static light scattering patterns for the suspensions of a serial Re at 5 mM EggPC. The *closed circle* shows experimental data and the *solid line* theoretical values as described in the text

cholate, the scattering spectra for bilayers bent upward, such as at Re = 0.3 and 0.38. Other series, as shown in Fig. 6, had similar scattering patterns after 48 h. Those different patterns indicate that the changes in the morphologies and properties of lipid aggregates depend on the detergent concentrations and also on time. The morphology of the lipid aggregates for the intermediate has been studied by SANS (small angle neutron scattering), SAXS (small angle x-ray scattering) as well as QLS (quasielastic light scattering) and some different aggregate structures such as disc or cylindrical micelles have been reported [8, 9, 31]. In the present SLS measurement, we tried many models to fit the experimental data and found an appreciate shell model for vesicles and a cylinder model for the intermediates.

Effects of interparticular structure factor on the fitting curves for vesicles

The scattered light intensity curves for the vesicle suspensions showed patterns with the characteristic interparticular structure in low q region. As shown in Fig. 7, if we used only the shape factor P(q) for the normal spher-

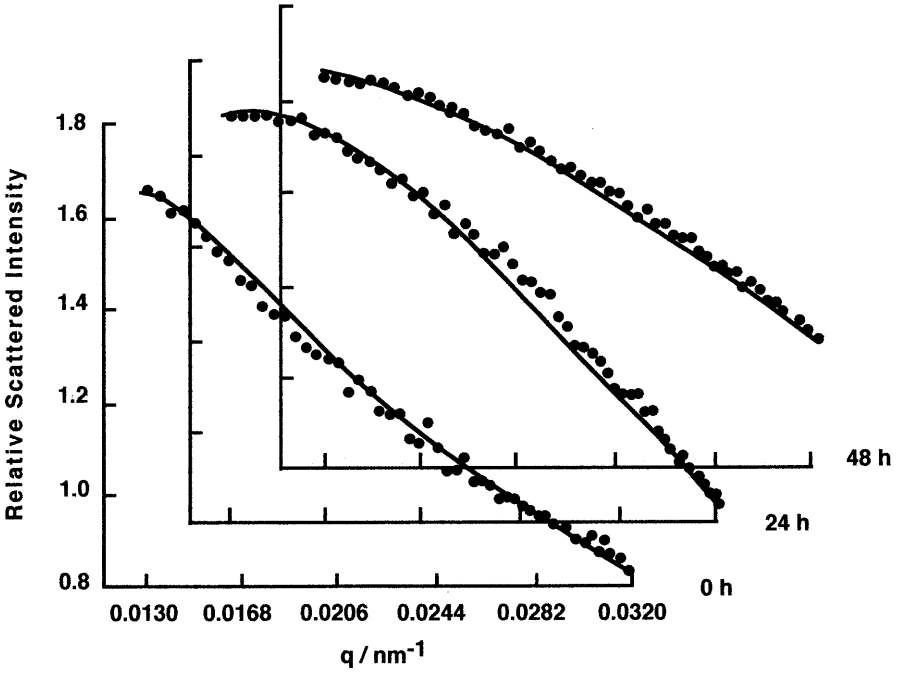

Fig. 6 Static light scattering patterns for the suspensions of 0 h, 24 h and 48 h at Re = 0.3. The *closed circle* shows experimental data and the *solid line* theoretical values as described in the text

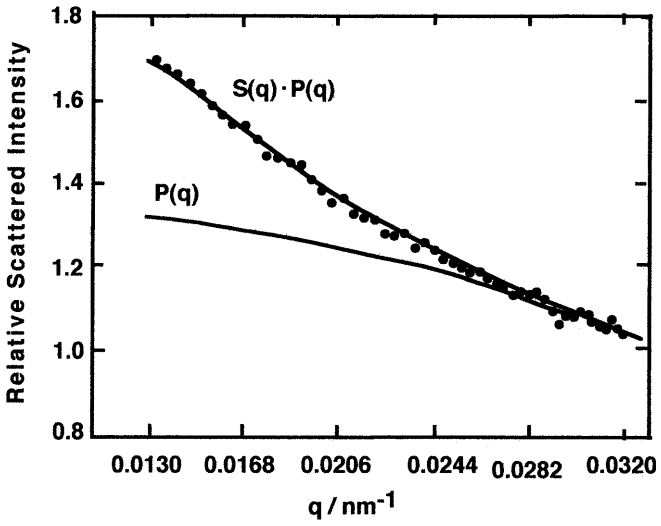

Fig. 7 Angular dependency of the intensities of the scattered light in Re = 0.15 and 5 mM EggPC. The experimental values are shown with *closed circles* and the theoretical ones are shown with *open circles* calculated by assuming two concentric spherical shell models, where P(q) is the spherical particle factor and S(q) is the intermolecular interference factor

ical shell model, the experimental scattering curves fit the theoretical one only in the larger q portion, but not in the smaller q region. Interpretation of the deviation from the theoretical curve would be due to the interparticular structure factor S(q) taking into account the intervesicular positional correlation. S(q) can be defined in terms of the particle pair correlation function g(R) as a function of the fractal dimension of the particle distribution in space (D) and interparticle correlation length (L).

In the region of vesicles, intensity over the entire q range could be approximated as two uniform concentric spherical shell models modified by considering the S(q) with different scattering lengths. Each spherical portion is expressed with the normal spherical particle factor P(q). The bilayer width was 4 nm. First the parameters of P(q) were fixed to fit the data in the entire q region as close as possible, and then S(q) was introduced with two other parameters D and L as mentioned above. All parameters were modified slightly to make the fit better over the whole q region. Both theoretical and experimental values agreed well in the entire q region, as shown in some fitting figures.

Characterization of SUV* using fractal dimension and interparticle correlation length

The parameters of R, D, and L obtained are shown in Table 1. In this experiment, the fitted parameter of the outer radius R was 23 nm. When sodium cholate was added, no significant change in size was shown,

Table 1 R, D, and L for the containing sodium cholate

Fitting data	*Re*					
	0	0.07	0.15	0.22	0.25	0.30*
R/*nm*	23	27	28	28	29	26
D	2.0_4	2.0_3	2.0_4	2.0_2	2.0_2	2.0_3
L/*nm*	101	105	120	120	128	60

*The coexistance of vesicles and micelles

indicating that the addition of sodium cholate did not affect the vesicle size. This result was compatible with the Z_{45} change. These R values for the vesicles were also significantly consistent with results from the QLS measurement. With increasing Re, the interparticle correlation length L of the vesicles gradually increased and reached 128 nm for SUV*. This behavior is related to the change in vesicle properties caused by the incorporation of sodium cholate. The increase in L would probably be caused by the repulsive electrostatic interaction of those vesicles containing sodium cholate due to an anion detergent. On the other hand, the fractal dimension D decreased gradually with the increase of Re. Where D = 3, the spheres are in a compact arrangement similar to three-dimensional packing of molecules in liquids. The special case of D = 2 is the Ornstein-Zernike form of the structure factor familiar in critical scattering from liquids [32]. In general, D can be a fractal number less than 3. Herein, the physical meaning of fractal dimension D would refer to the molecular packing behaviors of the vesicular membrane. The decrease in D indicates that the incorporation of sodium cholate affected the molecular packings of the EggPC membrane, leading to a high membrane fluidity. This would agree well with the result reported by Nichols, in which the incorporation of sodium cholate increased the rate of spontaneous phospholipid transfer between vesicles and altered the dissociation and/or association rate constants for phospholipid monomer-vesicle interaction [33]. SUV* had the smallest fractal dimension in the vesicle region, indicating weak molecular packings of the membrane. However, the weak molecular packings did not cause the SUV* fusion because of electrostatic repulsion of cholate-incorporated vesicles.

Effect of sodium cholate on zeta potential of the vesicles

To clarify further that the increase of interparticle correlation length and absence of fusion event were results of the repulsive interaction between SUV*, we measured zeta potential on those vesicles by ELS. Zeta potential is shown as a function of the molar ratio (Re) in Fig. 8. The zeta potential increased gradually with Re followed by a relatively great increment for SUV*. Apparently, the SUV* has distinct properties from other small

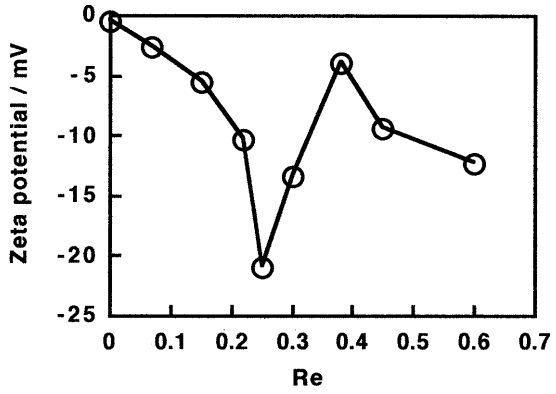

Fig. 8 Zeta potential of the vesicles or micelles as a function of the molar ratio Re

vesicles containing sodium cholate. The difference between SUV* and other vesicles would probably correspond to the partition behavior of sodium cholate between membrane and water phases. The surface charges were intensified with the increase of Re due to sodium cholate, an anionic detergent. As a result, SUV* had the highest surface electrostatics in those mixed vesicles.

Possible structure of the intermediate from the SLS measurement

In the region of intermediates, a smooth increase in the scattering curve was observed over the q region. For samples in this region the data could not be reasonably fitted by assuming that the measured scattering intensity was the sum of the intensity of a mixture of intermediates and vesicles or micelles. We tried to best fit with either the shell model or the hollow cylinder model to overlay the scattering intensity. Although the 0 h sample of Re = 0.3 fitted adequately with the shell model, the 24 h sample approached concomitantly neither the shell model nor the cylinder model, but the 48 h sample fitted rigorously with the cylinder model, as shown in Fig. 5 and Tables 1 and 2. The model fittings to three time-dependent samples reflect a slow structure transition of aggregate shapes, from vesicles to intermediates.

The cylinder dimensions determined from the most optimum fits are shown in Table 2. In this approach, a cylindrical shape of bilayers was suggested. The shape change and the increment of the bilayer dimension are time-dependent. Evolution of aggregate structures in vesicle solubilization depends on the nature of detergent, the methods used, and the experimental conditions and various aggregate structures will be found. This result emphasizes that caution should be maintained in deriving complicated structural models from static light scattering alone.

Table 2 Dimensions of the cylinder-like aggregates derived from the fitting the SLS data

Time/h	Fitting data	*Re*			
		0.3	0.38	0.45	0.60
0	R/nm			20	20
	R_i/nm			16	16
	H/nm			58	58
24	R/nm		20	19	
	R_i/nm		16	15	
	H/nm		50	83	
48	R/nm	20	19	19	
	R_i/nm	16	15	15	
	H/nm	55	67	108	

Conclusion

The vesicle sizes obtained by SLS agreed with the results of QLS measurement. The cylinder dimensions of the intermediates were determined by fitting to a hollow cylinder model. Furthermore, with the help of the quaternary structure factor, the SLS measurement was extended to the vesicle behaviors so that the aggregate structures and properties of SUV* could be characterized. The experimental results from SLS showed that SUV* had a high membrane fluidity and a strong repulsive interaction which distinguished them from other vesicles. The observed zeta potential for the small vesicles containing sodium cholate suggested that the repulsive interaction might result from an electrostatic repulsion between SUV* due to an anionic detergent. Although SUV* had a weak molecular packing of the membrane, the electrostatic repulsion hindered SUV* fusion, leading to the formation of small vesicles upon the removal of sodium cholate from the mixed micelles of sodium cholate and phospholipid.

References

1. Schubert R, Schmidt KH (1980) Biochemistry 27:8787
2. Devaux PF, Seigneuret M (1989) J Colloid Interface Sci 119:371
3. Otten D, Lobbecke L, Beyer K (1995) Biophys J 68:584
4. Walter A, Vinson PK, Kaplun A, Talmon Y (1991) Biophys J 60:1315
5. Ueno M, Akechi Y (1991) Chem Lett 1801
6. Ueno M, Kashiwagi H (2000) J Jpn Oil Chem Soc 49:1131

7. Carion-Travella B, Chopineau J, Ollivon M, Lesieur S (1998) Langmuir 14:3767
8. Long MA, Kaler EW, Lee SP (1994) Biophys J 67:1733
9. Small DM, Bourges MC, Dervichian DG (1966) Biochim Biophys Acta 125:563
10. Walter A, Vinson PK, Kaplun A, Talmon Y (1991) Biophys J 60:1315
11. Andrieux K, Forte L, Keller G, Grabielle-Madelmont, Lesieur S, Paternostre M, Ollivon M, Bourgaux C, Lesieur P (1998) Prog Colloid Polym Sci 110:280
12. Almog S, Kushnir T, Nir S, Lichtenberg D (1986) Biochemistry 25:2597
13. Levy D, Gulik, A, Seigneuret M, Rigaud J L (1990) Biochemistry 29:9480
14. Ueno M (1993) Membrane 18:96 (1993)
15. Ollivon M, Lesieur S, Grabielle-Madelmont C, Paternostre M (2000) Biochim Biophys Acta 1508:34
16. Lasch J (1995) Biochim Biophy Acta 1241:269
17. Ueno M, Kashiwagi H, Hirota N (1997) Chem Lett 217
18. Rotenberg M, Lichtenberg D (1991) J Colloid Interface Sci 144:591
19. Hjelm RP, Thiyagarajan P, Alkan-Onyuksel H (1992) J Phys Chem: 96:8653
20. Chang CS, Colbow K (1976) Biochim Biophys Acta 436:260
21. Ishigami Y, Gama Y, Sano Y, lang S, Wagner F (1994) Biotechnology Lett 16:593
22. Chen SH, Texeira J (1986) Phys Rev Lett 57:2583
23. Ishigami Y, Osman M, Nakahara H, Sano Y, Matsumoto M (1995) Colloids and Surfaces B: Biointerfaces 4:341
24. Ueno M (1989) Biochemistry 28:5631
25. Ames BN (1966) Methods Enzymol 8:115
26. Ueno M, Tanaka N, Horikoshi I (1989) J Membrane Sci 41:269
27. Sano Y (1988) J Colloid Interface Sci 124:403
28. Sano Y (1993) Biopolymers 33:69
29. Sano Y (1990) J Colloid Interface Sci 139:14
30. Oseki S (1982) Hyomen 20:632
31. Mazer NA, Benedek G B, Carey MC (1980) Biochemistry 19:601
32. Sinha SK, Freltoft T, Kjems J (1984) In: Family F, Landau, DP (eds) Kinetics of aggregation and gelation.. Elsevier Press, Amsterdam
33. Nichols JW (1986) Biochemistry 25,4596